Pramāṇa, Vol. 23, No. 2, August 1984, pp. 187–198. © Printed in India.

Calibration of different plastic track detectors using accelerated heavy ions

S M FARID

Department of Physics, Rajshahi University, Rajshahi, Bangladesh

Abstract. Measurements of the dependence of track etch rate on the energy-loss of different ions have been presented. In this method, $^{40}_{18}$Ar, $^{22}_{10}$Ne, $^{16}_{8}$O and $^{12}_{6}$C-ions of different energies are used as energetic heavy ions for track formation in the detectors. The bulk etch rate and track etch rate are measured for different temperatures and hence the activation energies are determined. The variation of $V = V_t/V_b$ along the trajectory of the track has been shown for different temperatures. The maximum etched track length is compared with the theoretical range as well as with the range reported earlier. The experimental results indicate the absence of a well-defined threshold in the plastics studied.

Keywords. Solid state nuclear track detectors; bulk etch rate; track etch rate; activation energy; calibration curve; threshold criterion.

PACS No. 29·40 – n

1. Introduction

The production of tracks by energetic ions in solid state nuclear track detectors (SSNTD) and the subsequent revealing of these tracks by chemical etching is widely used to detect and identify ions. The track etch rate, V_t, along the trajectory of a particle in the track detector is an increasing function of the energy deposited around the track. For particle identification with nuclear track detectors, it is essential to know the relation between the track etching rate and the energy deposited along the trajectory of the particle under a certain etching condition. The curve of the etching rate as a function of the deposited energy is often called a 'calibration curve'. The present study measures the track etch rate, V_t and range R of heavy ions having high energies by the track length method (Benton 1968; Dwivedi and Mukherji 1979; Farid and Sharma 1983). The calibration curves of different plastic detectors are drawn and the maximum etched track lengths of different ions are compared with the theoretical range obtained using range and stopping power equations of Mukherji and Nayak (1979). The dependence of bulk etch rate and track etch rate on etching temperature has also been studied.

2. Experimental procedure

Exposures of Mylar and polycarbonate (Makrofol-E and Lexan) plastic track detectors to different ions have been obtained from the cyclotron at JINR, Dubna (USSR). The ions and their energies are shown in table 1. The angle of exposure is 30° in all cases. All etching is carried out in $(6 \pm 0{\cdot}05)$N NaOH solution kept at constant temperature. The temperature at which etching takes place is kept constant to $\pm 0{\cdot}5$°C. The measure-

Table 1. Plastic detectors and ions used.

Detector material	Ion and energy (E = MeV/N)
Makrofol-E	$^{40}_{18}Ar$, $E = 7{\cdot}5$
polycarbonate	$^{22}_{10}Ne$, $E = 5{\cdot}5$
($C_{16}H_{14}O_3$	$^{16}_{8}O$, $E = 5{\cdot}5$
and $\rho = 1{\cdot}20$ g/cm^3)	$^{12}_{6}C$, $E = 5{\cdot}5$
Lexan	$^{40}_{18}Ar$, $E = 7{\cdot}5$
polycarbonate	$^{22}_{10}Ne$, $E = 7{\cdot}7$
($C_{16}H_{14}O_3$	$^{16}_{8}O$, $E = 8{\cdot}7$
and $\rho = 1{\cdot}20$ g/cm^3)	$^{12}_{6}C$, $E = 8{\cdot}7$
Mylar	$^{40}_{18}Ar$, $E = 7{\cdot}5$
($C_{10}H_8O_4$ and	$^{22}_{10}Ne$, $E = 7{\cdot}7$
$\rho = 1{\cdot}39$ g/cm^3)	$^{16}_{8}O$, $E = 8{\cdot}7$

The angle of exposure with respect to detector surface was 30°.

ments are taken with an 'Olympus' microscope having an eyepiece micrometer of least count LC = 0·215 μm at a magnification of 900 ×.

3. Results and discussions

3.1 *Etching temperature on V_b*

The bulk etch rates of Mylar and polycarbonate detectors have been measured by two methods (Dwivedi and Mukherji 1979; Enge *et al* 1975) viz (i) track diameter method, and (ii) gravimetric method. The bulk etch rate is determined at 50, 60, 70, 80 and 90°C for 6 N NaOH solution. Both the methods give the same results within the limits of uncertainty of the measurements which shows the isotropic etching character of mylar and polycarbonate plastic detectors. The results are presented in figure 1. The dependence of V_b on etching temperature, T (in absolute scale) is exponential and can be expressed by the relation:

$$V_b = A \exp(-E_b/kT)$$

where A is a constant, k is the Boltzmann constant and E_b is the activation energy for bulk etching. From the slopes of the straight lines, the E_b values are calculated and are presented in table 2.

3.2 *Etching temperature on V_t*

When an exposed sample is etched in NaOH solution conical tracks are observed. The intersection between a conical track and the etched surface is an ellipse with the track position shifted away from the centre towards the track tip. The major and minor axis diameters are measured. The projected track length, l is measured from the centre of the track ellipse at the etched surface to the end of the track tip. The corrected projection length, l_p is determined by considering the geometry of tracks as suggested by Benton

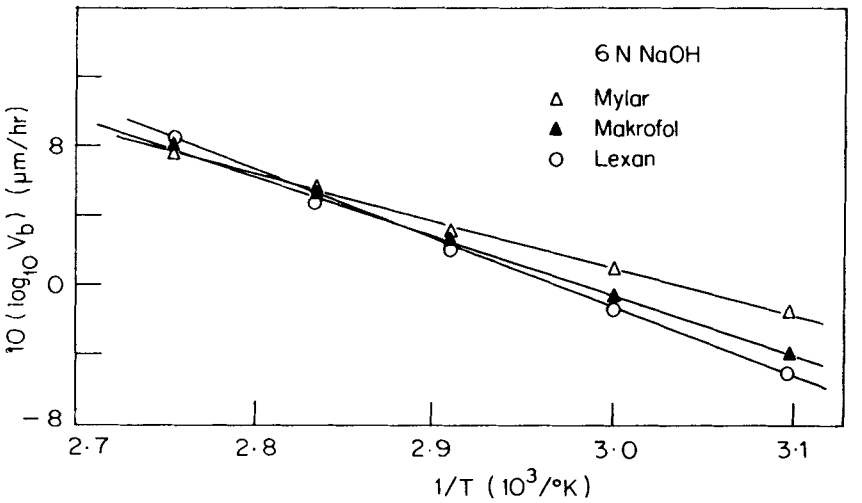

Figure 1. Variation of V_b of Makrofol, Lexan and Mylar plastic detectors with etching temperature for 6 N NaOH solution.

Table 2. Activation energy for bulk etching of different plastic detectors.

Detector	Activation energy for bulk etching, E_b (eV)
Makrofol-E	0·72 ± 0·06
Lexan	0·71 ± 0·06
Mylar	0·54 ± 0·05

The chemical etchant was 6 N NaOH.

(1968). The true track length, L (the length from the original surface to the terminal end of the track) is calculated by the relation (Benton 1968; Dwivedi and Mukherji 1979; Farid and Sharma 1983).

$$L = (l_p/\cos\delta) + (V_b t/\sin\delta) - V_b(t - t_c) \tag{1}$$

where δ = angle of incidence; $V_b t/\sin\delta$ = the surface etching correction and t_c is the time required to etch the tracks up to the point where they stop (etched until the track ends become round).

V_t is calculated by the relation (Dwivedi and Mukherji 1979; Farid and Sharma 1983)

$$V_t = \Delta L/\Delta t \tag{2}$$

where ΔL is the track length increase in the etching time Δt.

Samples of Makrofol exposed to $^{22}_{10}$Ne and $^{40}_{18}$Ar-ions are etched in 6 N NaOH at 70°C. At least 50 tracks are measured for each set of observations. The variation of l_p and L with etching time for $^{22}_{10}$Ne and $^{40}_{18}$Ar-ions are shown in figure 2. It is observed that the projected length starts decreasing after complete etching time, t_c. When the bulk etching and over-etching corrections are made the true track length remains constant beyond t_c as can be seen from figure 2. Similar curves drawn for $^{16}_{8}$O and $^{12}_{6}$C

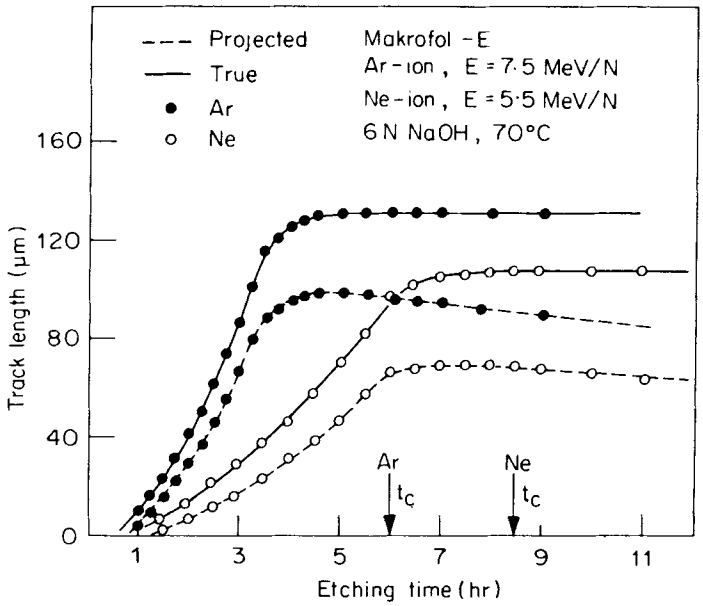

Figure 2. Variation of (**a**). projected track lengths and (**b**). true track lengths of $^{40}_{18}$Ar and $^{22}_{10}$Ne-ions in Makrofol-E with etching time.

ions in Makrofol are not shown. Using (2), the V_t values at different points on the track are obtained from figure 2. Figure 3 shows the variation of V_t with residual range of different ions in Makrofol for etching in NaOH at 70°C. Clearly V_t increases with penetration depth. Following the same procedure, V_t is calculated for different ions in Lexan and Mylar. Figure 4 shows the variation of V_t with residual range of different ions in Lexan for 70°C. The same plot for different ions in Mylar is shown in figure 5 for 6 N NaOH at 60°C.

Similarly the plots of V_t *vs* residual range of different ions in Makrofol and Lexan are drawn for etching temperatures of 50, 60, 80 and 90°C. The same plots for different ions in Mylar are also drawn for temperatures of 30, 40, 50 and 70°C. These plots which are similar in nature to those shown in figures 3, 4 and 5 are not presented here. The V_t value corresponding to a particular residual range (50 μm in the present case) is obtained from these curves for different temperatures. The effect of temperature on V_t is shown in figure 6 for different ions in Makrofol-E. The rise of V_t with etching temperature, T (in absolute scale) is exponential and can be expressed by $V_t = B \exp(-E_t/kT)$, where B is a constant and E_t is the activation energy for track etching. The E_t values are calculated from the slopes of the straight lines in figure 6 for the different ions in Makrofol-E. These are presented in table 3. The V_t *vs* $1/T$ plots for different ions in Lexan and Mylar show similar exponential dependence of V_t on T. The E_t values for different ions in Lexan and Mylar are also presented in table 3. The activation energy for track etching is constant for different ions in a particular detector but is different for different plastics, being the characteristic of the detector material. Again it is noted that $E_b \simeq E_t$ for the detectors under study.

The cone angle values given by $\sin\theta = V_b/V_t$ have been determined for different ions in a detector from the experimentally determined V_b and V_t values. The variation of cone angle, θ with etching temperature is shown in figure 7 for different ions in

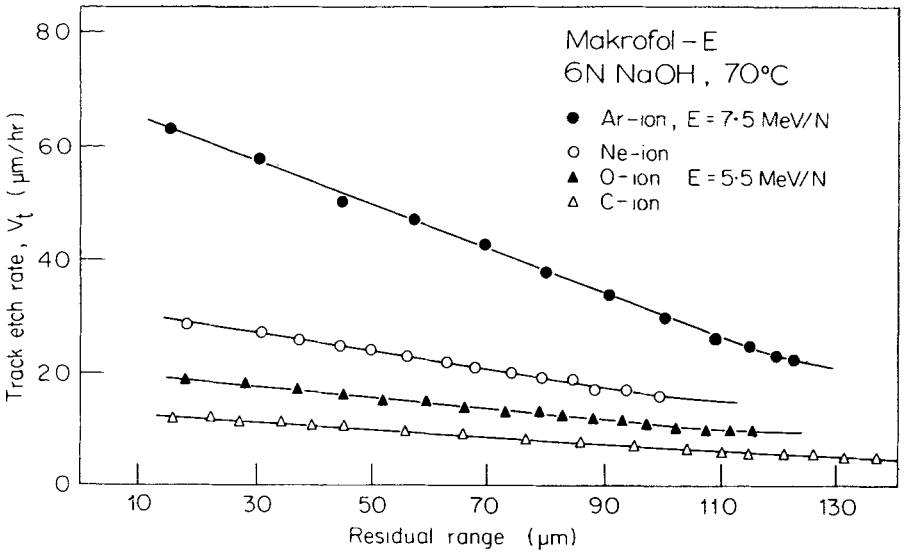

Figure 3. Variation of V_t with residual range of different ions in Makrofol-E plastic detector.

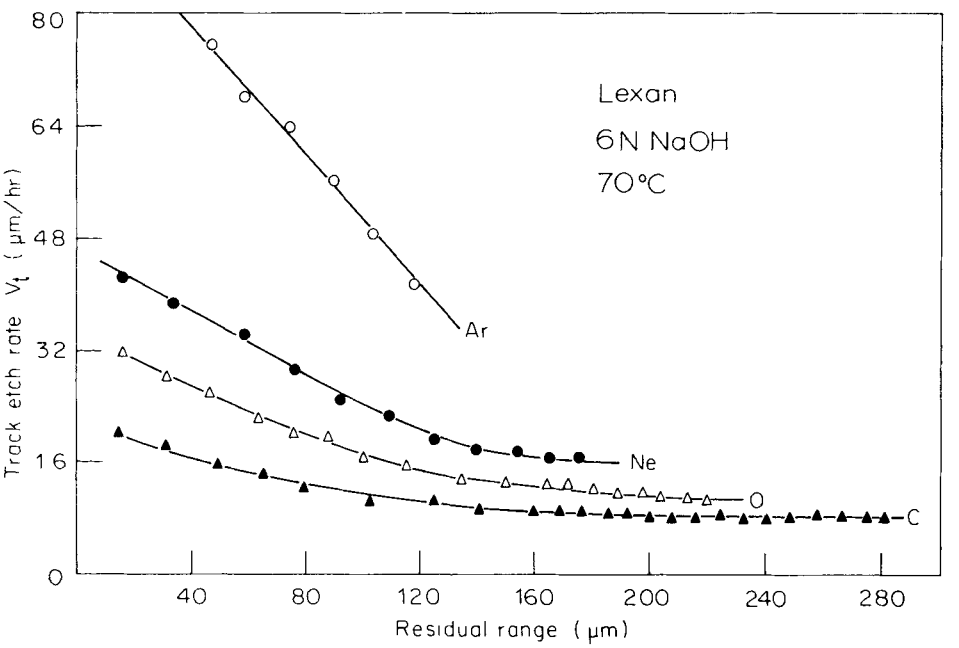

Figure 4. Variation of V_t with residual range of different ions in Lexan detector.

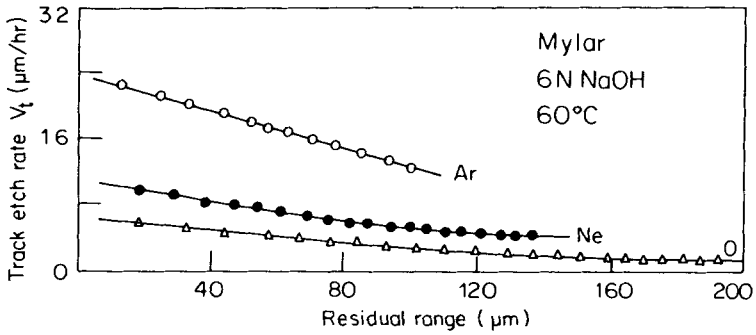

Figure 5. Variation of V_t with residual range of different ions in Mylar detector.

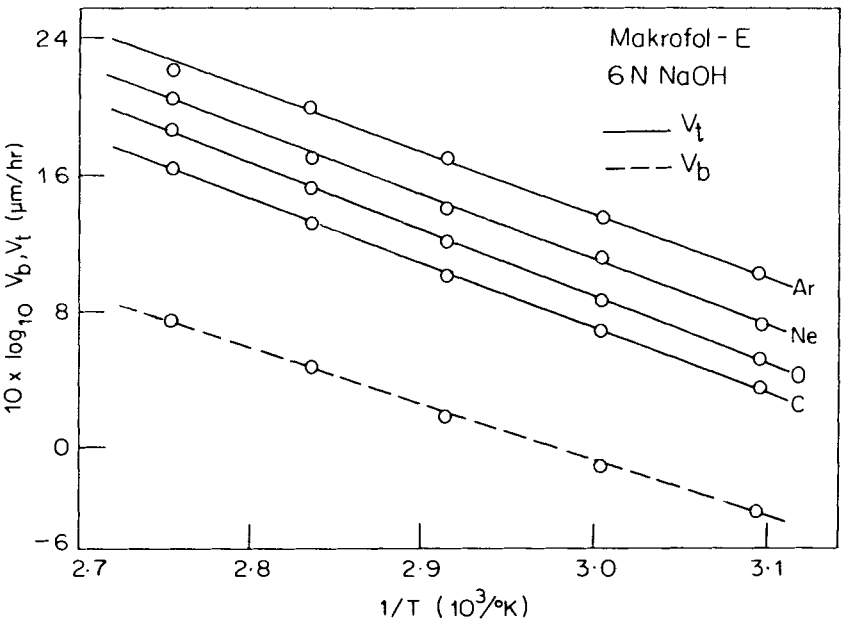

Figure 6. Dependence of V_t on the etching temperature for different ions in Makrofol-E detector.

Table 3. Activation energy for track etching of different ions in plastic detectors.

	Activation energy, E_t (eV) for			
Detector	C	O	Ne	Ar
Makrofol-E	0·68 ± 0·07	0·66 ± 0·07	0·65 ± 0·07	0·64 ± 0·07
Lexan	0·66 ± 0·07	0·66 ± 0·07	0·64 ± 0·07	0·63 ± 0·07
Mylar	—	0·49 ± 0·05	0·47 ± 0·05	0·49 ± 0·05

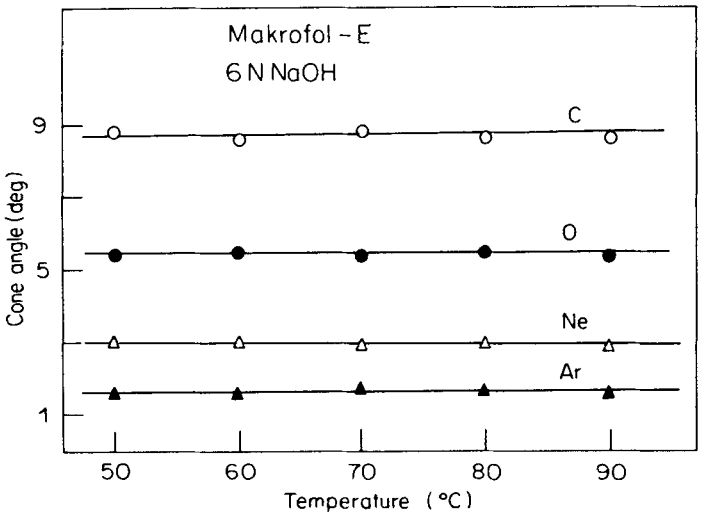

Figure 7. Dependence of cone angle θ on the etching temperature for different ions in Makrofol.

Makrofol. The cone angle of a heavier ion is smaller than that of a lighter ion at a particular temperature (figure 7). Again the cone angle, θ of a particular ion remains constant between etching temperatures 50°C and 90°C for Makrofol-E. The same conclusions are also valid for Lexan and Mylar.

Thus in etching tracks of light and heavy ions, it is observed that tracks of heavy particles etch faster (figures 3–5) results in the tracks having correspondingly smaller cone angles (figure 7). For a given etch time, the tracks also have correspondingly longer track lengths (figure 2).

3.3 *Evaluation of V_t along the trajectory of the particle*

In figure 8 data of the excess track etch rate ratio, $(V-1)$ are plotted *vs* the residual range of $^{40}_{18}$Ar-ion in Makrofol-E for different temperatures. It is noted that all the points belong to the same curve within the accuracy of the measurements. The solid curve is the best fit to the experimental points. The best fitted curves to the experimental points for Ne, O and C are also presented in the same figure. It is concluded that V_t along the particle trajectory depends on the etching temperature but the normalized track etch rate, $V = V_t/V_b$ is independent of the etching temperature. The same conclusion is also valid for Lexan and Mylar detectors and hence $V(R)$ curves of different ions in Lexan and Mylar are not shown here.

The $V(R)$ curve deduced from our study approaches the $V = 1$ value (threshold criterion) asymptotically which clearly indicates the absence of a well-defined threshold in the plastics studied. Somogyi *et al* (1976) and Dartyge *et al* (1977) have made similar remarks after investigating alpha-particle tracks in different plastic detectors and heavy ion tracks in crystal detectors respectively.

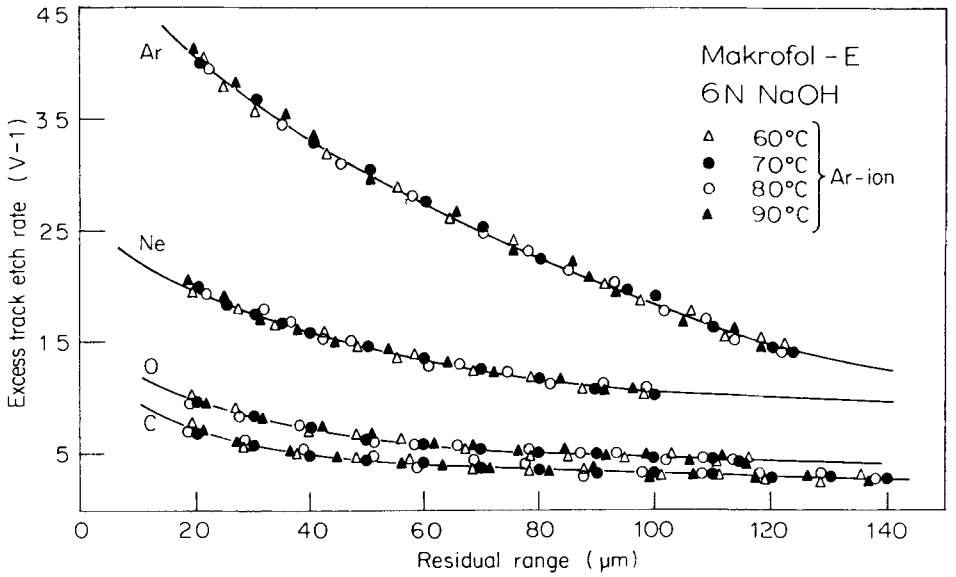

Figure 8. Variation of excess track etch rate, $(V-1)$ with residual range of different ions in Makrofol for different etching temperatures.

3.4 *Range of different ions in mylar and polycarbonate detectors*

Exposed samples of Makrofol, Lexan and Mylar are etched in 6 N NaOH at 70°C. The average length of maximum etched tracks (etched until the tips of the tracks become round) is calculated for different ions. The results are presented in table 4. The range and stopping power equations of Mukherji and Nayak (1979) have been used to calculate the theoretical ranges of different ions. The ranges of different ions in Makrofol-E and Lexan and in Mylar are computed. The computer lists the specific energy-loss, dE/dx and the penetration depth (*i.e.* range) starting from the intial ion energy down to zero at intervals of $\delta E(\delta E = 0{\cdot}01$ MeV). The computed ranges of different ions are also given in table 4. The maximum etched track lengths agree with the theoretical ranges to better than 2%. Benton (1968) using restricted energy-loss (REL) criterion for track formation in polymers computed the ranges of different ions in plastic detectors. Tripier *et al* (1974) used the equations of Barkas and Heckman which are originally valid for nuclear emulsions with some modifications for calculating the ranges of different ions in plastic detectors. The present values of ranges of different ions agree closely with the corresponding ranges reported by Benton (1968) and Tripier *et al* (1974). Hence the range and stopping power equations of Mukherji and Nayak (1979) can be used for calculating the ranges of heavy ions in complex media.

3.5 *The calibration curve*

Using the values obtained from the computer output, the plots of specific energy-loss, (dE/dx) *vs* residual range have been drawn for different ions in Makrofol, Lexan and Mylar (not shown). The variation of V_t with residual range is shown in figures 3–5. Combining these figures, the 'calibration curves' $[(dE/dx)$ *vs* $V_t]$ of Makrofol, Lexan and Mylar are shown in figures 9–11 for different etching temperatures. In figure 12,

Table 4. Calculated (R_{cal}) and experimental (R_{expt}) ranges of various ions in different plastic detectors.

Detector	Ion	Energy (MeV/N)	R_{expt} (μm)	R_{cal} (μm)
Makrofol-E	$^{40}_{18}$Ar	7·5	130·74 ± 2·80	132·96
	$^{22}_{10}$Ne	5·5	107·52 ± 2·20	109·63
	$^{16}_{8}$O	5·5	123·25 ± 2·50	125·22
	$^{12}_{6}$C	5·5	145·55 ± 2·95	147·93
Lexan	$^{40}_{18}$Ar	7·5	132·46 ± 2·42	134·40
	$^{22}_{10}$Ne	7·7	190·50 ± 2·86	194·26
	$^{16}_{8}$O	8·7	242·22 ± 3·28	246·85
	$^{12}_{6}$C	8·7	301·44 ± 4·23	306·88
Mylar	$^{40}_{18}$Ar	7·5	112·50 ± 3·24	114·26
	$^{22}_{10}$Ne	7·7	150·56 ± 3·46	153·50
	$^{16}_{8}$O	8·7	210·50 ± 4·28	214·51

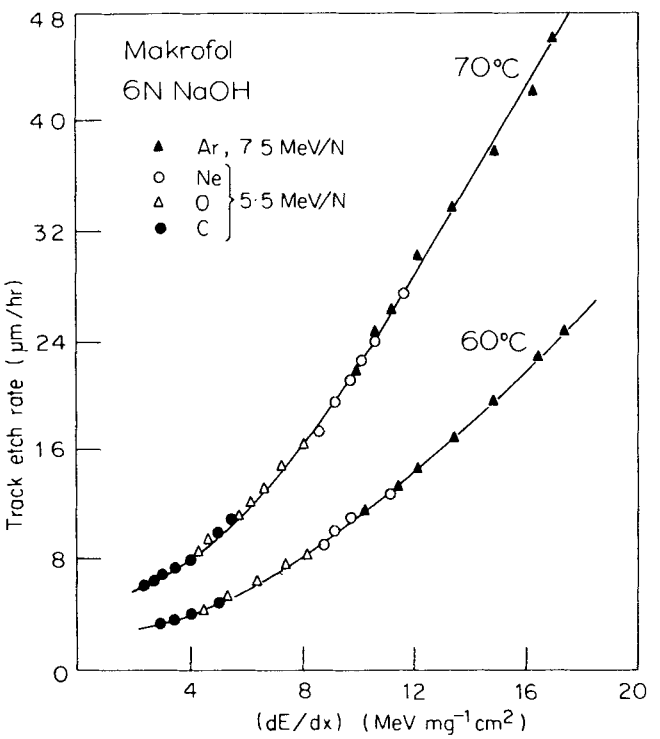

Figure 9. Dependence of V_t on the specific energy-loss dE/dx of different ions in Makrofol for 60°C and 70°C.

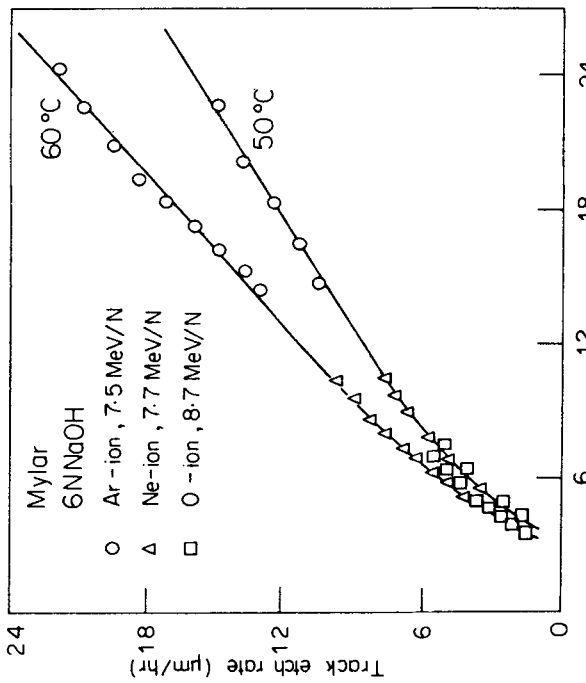

Figure 11. Dependence of V_t on the specific energy-loss, dE/dx of different ions in Mylar for 50°C and 60°C.

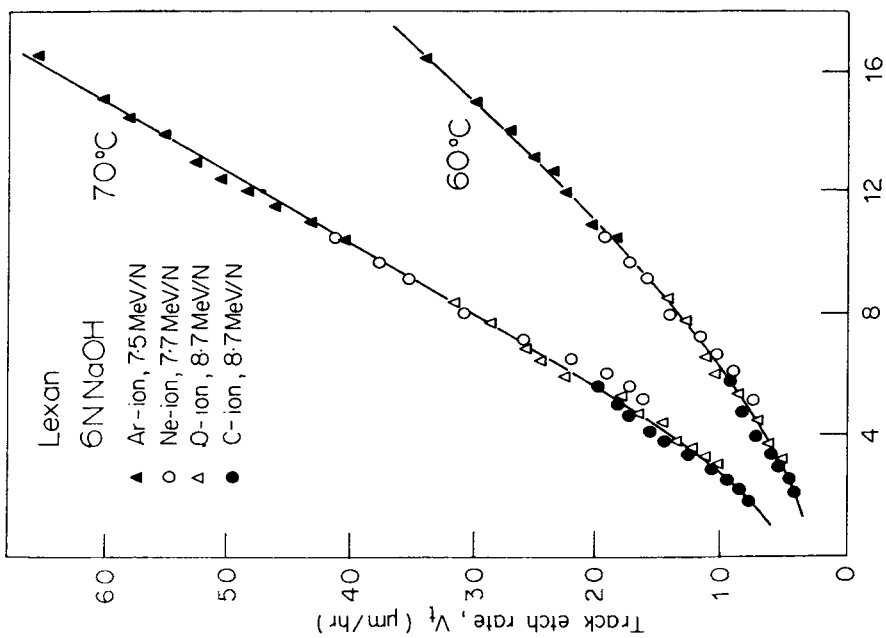

Figure 10. Dependence of V_t on the specific energy-loss, dE/dx of different ions in Lexan for 60°C and 70°C.

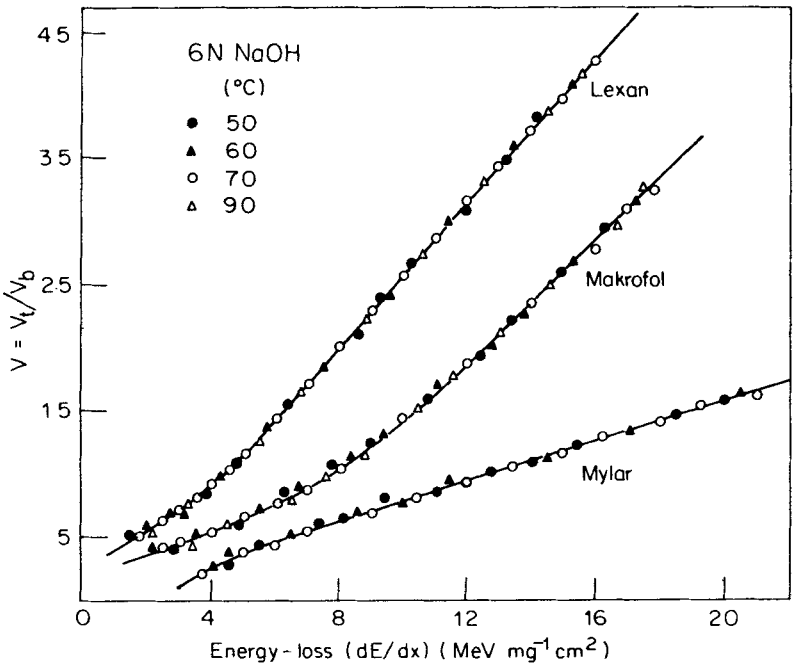

Figure 12. Dependence of $V = V_t/V_b$ on the specific energy-loss, dE/dx of different ions in Makrofol, Lexan and Mylar for different etching temperatures.

Table 5. Values of the parameters α and β for different plastic detectors.

	Parameters of $V = 1 + \alpha(dE/dx)^{\beta}$	
Detector	α	β
Makrofol-E	0·027	3·19
Lexan	0·030	3·12
Mylar	0·003	3·27

The chemical etchant was 6 N NaOH.

the normalized track etch rates are plotted against (dE/dx) of different ions in Makrofol, Lexan and Mylar. The interesting conclusion is that for all the detectors studied V_t depends on (dE/dx) as well as on etching temperature. But the normalized track etch rate depends only on (dE/dx) and not on the etching temperature. The solid curves in figure 12 are the best fit to the experimental points. These curves can be well described by the relation (Enge *et al* 1975; Somogyi *et al* 1976; Somogyi 1980)

$$V = 1 + \alpha(dE/dx)^{\beta},$$

where α and β are fitting parameters characterizing the detector materials and the track etching conditions employed. The values of these parameters are calculated using computer fitting. They are presented in table 5. The α and β values obtained by Somogyi

Table 6. Values of the parameters α and β for different plastics obtained (Somogyi *et al* 1976).

Detector	Etching conditions (at 70°C)	Parameters of $V = 1 + \alpha(dE/dx)^{\beta}$	
		α	β
Makrofol-E	15 g KOH + 45 g H_2O + 40 g C_2H_5OH	0·027	2·84
Lexan	30% KOH	0·019	2·92
Mylar	30% KOH	0·002	3·27

et al (1976) for different detectors using different etching conditions are shown in table 6 for comparison.

Thus the recently developed range and energy-loss equations of Mukherji and Nayak (1979) which are easy to handle and do not contain any arbitrary parameters can also be used for calculating the energy-loss and range of heavy ions in complex media like Makrofol, Lexan and Mylar.

References

Benton E V 1968 *Study of charged particle tracks in cellulose nitrate* USNRDL-TR-68-14
Dartyge E, Duraud J P and Langevin Y 1977 *Rad. Eff.* **34** 77
Dwivedi K K and Mukherji S 1979 *Nucl. Instrum. Meth.* **161** 317
Dwivedi K K and Mukherji S 1979 *Nucl. Instrum. Meth.* **159** 433
Enge W, Grabisch K, Dallmeyer L, Bartholoms K P and Beaujean R 1975 *Nucl. Instrum. Meth.* **127** 125
Farid S M and Sharma A P 1983 *Pramana* **21** 339
Farid S M and Sharma A P 1983 *Rad. Eff.* **80** 121
Mukherji S and Nayak A K 1979 *Nucl. Instrum. Meth.* **159** 421
Somogyi G, Grabisch K, Schezer R and Enge W 1976 *Nucl. Instrum. Meth.* **134** 129
Somogyi G 1980 *Nucl. Instrum. Meth.* **173** 21
Tripier J, Remy G, Ralarosy J, Debeauvais M, Stein R and Huss D 1974 *Nucl. Instrum. Meth.* **115** 29